Modeling and simulation for phase coarsening: A comparison with experiment

K. G. Wang, M. E. Glicksman, and K. Rajan
Materials Science and Engineering Department, Rensselaer Polytechnic Institute, Troy, New York 12180-3590, USA
(Received 10 December 2003; published 16 June 2004)

The phase coarsening of precipitates is modeled in the framework of Debye-Hückel theory. The interactions observed among a population of precipitates dispersed throughout a matrix can be described by diffusion screening. The relationship between the maximum particle radius and the volume fraction of the phases is established, and the rate of coarsening is related to the volume fraction and the self-similar particle size distribution. We simulated the dynamics of late-stage phase separation using multiparticle diffusion methods. Experimental measurements on the rates of coarsening of $\delta'(Al_3Li)$ precipitates in binary Al-Li alloys are compared with our results using modeling and simulation. The theoretically predicted particle size distributions and the maximum radius expected for particles in the microstructure agree well with recent experimental results.

DOI: 10.1103/PhysRevE.69.061507 PACS number(s): 64.75.+g, 64.60-i

I. INTRODUCTION

Phase coarsening is a common relaxation process during late-stage microstructural evolution that leads to a decrease in the excess total interfacial energy of two-phase systems. During phase coarsening, larger particles tend to grow by absorbing solute atoms at the expense of small particles that tend to dissolve by losing them. Over time, this "competitive diffusion" results in an increase in the average size of the particle population, and in a concomitant decrease in the number density of particles. Indeed, the physical and mechanical properties of two-phase materials, such as hardness and toughness, depend sensitively on the material's average particle size and particle size distribution function (PSD).

The statistical mechanics of phase coarsening was initiated by Lifshitz and Slyozov [1] and by Wagner [2]. This theory is often referred to as LSW theory, and retains full validity only in the limit of a vanishing volume fraction. The prediction of LSW theory that the cube of the average length scale of particles increases linearly with time is, however, shown to be valid by numerous experiments even in the case of finite volume fractions. Specifically, LSW found that in the long-time limit of phase separation the PSD exhibits self-similar (affine) properties, wherein the microstructure continuously changes by a single scale factor.

LSW ignored the effect of volume fraction of particles and the interaction among particles because they assumed that the neigboring particles are far away from the particle of interest. However, in real systems such as alloys, a finite volume fraction of particles V_V is distributed in close proximity, and many-body interactions arise among particles. Numerous attempts have been made over the past 40 years to improve upon LSW theory by extending its applicability to the more realistic situation of nonzero volume fractions. Ardell [3], for example, modified LSW theory to consider the effect of nearest neighbors on the growth rate of particles. Ardell's theory showed that the PSD broadened from the interactions and the coarsening rate increased with the volume fraction. His detailed results, however, overestimate the influence of the volume fraction and deviate considerably from more recent theories and computer simulations [4]. Variations of Ardell's method have been studied by Tsumuraya and Miyata [5] using a series of coarsening models, referred to as TM models. Specifically, these authors defined a "radius of influence" around each particle using six theoretical mean-field interactions, and studied the growth rates of the particles and the nature of the predicted PSD's. Two of the six models predicted broadening of the PSD's. Each of the six TM models, however, employed heuristic extensions of the basic LSW approach. Ardell's original model and the TM models all belong to the same universality class, and therefore share some common approximations and exhibit some similar traits.

Brailsford and Wynblatt [6] employed "effective medium" theory to study phase coarsening. They obtained growth rates of the particles and a broadened PSD, and established an implicit relationship between the coarsening rate and volume fraction. Marsh and Glicksman [7] then introduced the concept of a statistical "field cell" acting around each size class of the particles undergoing phase coarsening, and obtained coarsening rates that are in good agreement with data derived from liquid-phase sintering experiments, particularly in the range of volume fractions between $0.3 \leqslant V_V \leqslant 0.6$. All of the theoretical models mentioned above employed growth rate equations based on using Laplace's equation as the quasistatic approximation for the time-dependent diffusion field [8].

Marqusee and Ross [9], by contrast, limited the spatial extent of the Laplacian field by taking into account screening effects in active two-phase media containing a distribution of diffusion sources and sinks. Instead of Laplace's equation, Marqusee and Ross used Poisson's equation to derive a kinetic expression for the growth rate of particles. They obtained the maximum particle radii in systems at different volume fractions, the relationship between the coarsening rate and the volume fraction, and the affine (self-similar) PSD's. Following this approach, Fradkov *et al.* [10] and Mandyam *et al.* [11] studied coarsening kinetics in finite clusters using Poisson's equation to approximate the multiparticle diffusion. Their main focus was exposing the relationship between the diffusion screening length and the phase volume fractions at extremely low volume fractions.

More recently, Glicksman, Wang, and Marsh [12] solved the Debye-Hückel equation to obtain the growth rates of particles. Those authors established relationships between particle-particle interactions, the coarsening rates, and the volume fraction.

The earliest study of multiparticle diffusion during phase coarsening using numerical simulation was published in 1973 by Weins and Cahn [13], who used just a few particles in several configurations to demonstrate some basic coarsening interactions. Their work was followed by an investigation published by Voorhees and Glicksman [14] who systematically studied the behavior of several hundred particles randomly distributed in a periodic, three-dimensional unit cell to simulate microstructural phase coarsening. Later, Beenaker [15] further improved multiparticle diffusion simulation procedures and was able to increase the total number of particles during simulation to several thousand. Other investigators [16–18] continued to improve upon the accuracy and statistical basis of large-scale simulations of late-stage phase coarsening.

Baldan [19] reviewed the status of experimental studies on phase coarsening in nickel-base superalloys. Indeed, a great deal of experimental data currently exist for a variety of interesting high-temperature alloy systems. However, most superalloy systems and the conditions for the experiments applied to them differ from those that are optimal for modeling and simulation. To our knowledge the chief exception to this situation is that of phase coarsening of $\delta' - Al_3Li$ precipitates dispersed in binary Al-Li alloys. The two-phase binary alloys based on Al-Li provides a nearly ideal binary system for kinetic study, because the δ' particles in this alloy have a small lattice mismatch with the solid solution matrix phase, thus contributing a negligible amount of strain-induced free energy to the coarsening process. Mahalingam *et al.* [20] studied coarsening of $\delta' - Al_3Li$ precipitates in binary Al-Li alloys using quantitative transmission electron microscopy. Mahalingam *et al.* obtained steady-state PSD's and coarsening rates for microstructures having different precipitate volume fractions. Recently, Snyder *et al.* [21,22] studied the coarsening of solid-Sn particles in Pb-Sn eutectic liquid under microgravity condition. Their experimental PSD's, however, were judged as not reflecting steady-state phase coarsening.

All of the theories mentioned above have shown that a nonzero volume fraction of particles does not alter the temporal exponent in the coarsening law. However, changing the volume fractions does alter the coarsening rate, the kinetic coefficient of the growth law, and the resulting PSD. Despite this qualitative agreement, quantitative coarsening rates and PSD's differ from theory to theory [23]. The agreement found between theoretically predicted and experimentally measured volume fraction dependences of the PSD's and the coarsening rate is generally not satisfactory. Although many models and simulations of phase coarsening exist, as mentioned above, few provide predictions that compare quantitatively with experimental results. The chief reason for this disparity is that key assumptions required by many models and simulations are not satisfied by the experiments. In addition, the range of volume fractions that have been studied theoretically is not the same as that used experimentally. In this paper, we first extend our original diffusion screening model [12] to resolve the volume fraction dependences of the maximum particle radius, coarsening rate, and PSD during steady-state diffusion-mediated phase coarsening. Next, we simulate phase coarsening in microstructures reflecting the same volume fraction as used experimentally. Finally, we compare predictions based on modeling and simulation with experimental results, and make suggestions for future quantitative studies of late-stage phase coarsening.

The organization of this paper is as follows: In Sec. II, we briefly introduce the diffusion screening model of coarsening interactions and describe some results. In Sec. III, we provide details of recent multiparticle diffusion simulations. In Sec. IV, we compare predictions from modeling and simulation with experimental observations. Finally, in Sec. V, we conclude with discussion and a summary.

II. MODELING

An initial modeling of diffusion-limited phase coarsening was published in our previous paper [12]. However, in this section, we describe the differences with and improvements over prior modeling [12], and make the modeling more comprehensive. The spherical particle size is specified by the dimensionless radius R and its dimensionless volume per steradian V. All length scales are nondimensionalized through the appropriate capillary length, $l_c = 2\gamma V_m / R_g T$, and the coarsening time is nondimensionalized through the characteristic diffusion time $\tau_d = l_c / D C_0 V_m$ to yield the dimensionless time t where γ, V_m, D, C_0, R_g, and T represent the surface energy, molar volume, diffusivity, and solute concentration in the matrix phase at a planar interface, universal gas constant, and the absolute temperature, respectively. We adopt the usual mean-field ansatz that, at any instant in time, there exists a *critical* particle size such that the growth rate averaged over all particles having this size is zero. The critical radius of the population of particles is denoted by $R^\star(t)$, and the renormalized radius of a particle ρ is defined as its ratio $R/R^\star$.

The central challenge of any phase coarsening theory is to formulate an accurate expression for the renormalized particle growth rate $\dot{\rho}$ in each size class of the dispersoid population. Several studies suggest for microstructures with moderate volume fractions of the dispersed phase ($V_V \leqslant 0.3$), that there exists interactions among particles, and diffusive exchanges between them that depend on their relative sizes and spatial positions. Developing a detailed description of these particle-particle interactions would be prohibitively difficult for a microstructure comprised of a large number of different sized particles. The challenge is how best to simplify such a many-body system so that an accurate result is still obtained. One method of incorporating particle-particle interactions during late-stage phase coarsening, at least to first order, is to represent the individual interactions by a "diffusion screening length" R_0. The diffusion screening length—a collective property of the particle population—sets the range over which interactions occur, and beyond which they cease. The normalized diffusion screening length may be shown to be defined as $\rho_0 \equiv R_0 / R^\star$ [12].

To proceed with an analysis of a diffusionally screened coarsening system of polydisperse spherical particles suspended in a three dimensional matrix, one specifies the sizes of particles by the distribution $F(R,t)$, defined here as the total number of particles per unit volume at time t, with radii between R and $R+dR$. The emission of solute from dissolving particles, or its absorption by growing particles, is modeled mathematically by a distribution of *sources* or *sinks* throughout the two-phase microstructure. A consequence of the system being an "active medium" is that the spatial extent of the diffusion field surrounding the particles, on average, is restricted through diffusion screening. The onset of diffusive screening with any nonzero volume fraction requires that the Poisson equation replace the usual Laplacian approximation for quasistatic diffusion [8], which yields the diffusion analog of the Debye-Hückel equation, namely [10]

$$\nabla^2\varphi(\vec{\mathbf{r}}) - \kappa^2[\varphi(\vec{\mathbf{r}}) - \varphi_\infty] = 0, \tag{1}$$

where $\varphi(\vec{\mathbf{r}})=[C(\vec{\mathbf{r}})-C_0]/C_0$ defines a dimensionless potential. $C(\vec{\mathbf{r}})$ is the physical concentration field in the continuous matrix surrounding the particles, and $\kappa \equiv R_0^{-1}$ is introduced as the diffusion analog of the reciprocal diffusion screening length. φ_∞ is the pervading "background" diffusion potential in the matrix. Equation (1) is well known from theories of dilute ionic solutions and plasmas.

The general solution to the Debye-Hückel equation can be expressed in the form of the well-known Yukawa potential as [10]

$$\varphi(r) = A - \frac{B}{r}\exp(-\kappa r), \tag{2}$$

where A and B are constants, and r is the distance from the center of the ith particle to the field point. It should be noted that the term B/r in Eq. (2) corresponds to the unscreened Coulombic potential in three-dimensions, i.e., the spherical Laplacian potential. This Laplace potential is effectively "cut off" by the exponential term over the diffusion screening length. One can determine the constants A and B in Eq. (2) by using the Gibbs-Thomson local equilibrium relation at the surface of the ith particle, namely, $\varphi(R_i)=1/R_i$, and an additional boundary condition that specifies the outer potential at the diffusion screening distance, $\varphi(R_0)=1/R^\star$. One may now obtain the kinetic growth law of a spherical particle to first-order at small volume fractions by calculating the volume flux using the interfacial concentration gradient and the concentration jump specified by the phase diagram; specifically, one finds that

$$\frac{d\rho}{d\tau} = \frac{1}{K^\star}\frac{(\rho-1)}{\rho^2}\left(1+\frac{\rho}{\rho_0}\right) - \rho, \tag{3}$$

where

$$K^\star = \frac{1}{3}\frac{d(R^\star)^3}{dt}. \tag{4}$$

$K^\star$ is the coarsening rate constant for the critical size [12]. The dimensionless time variable τ is defined as

$$\tau \equiv \frac{1}{3}\ln(R^\star)^3. \tag{5}$$

The full details in deriving Eq. (3) were published in our previous paper [12]. The normalized diffusion screening length ρ_0 is related directly to the ratio of moments of the PSD and to the square root of the system's volume fraction as follows:

$$\rho_0 = \sqrt{\frac{\langle\rho^3\rangle}{3\langle\rho\rangle V_V}}. \tag{6}$$

Equation (6) clearly shows that the interactions among particles are explicitly related to the volume fraction parameter, and implicitly to the PSD through the moments of the affine (scale free) PSD. Marsh and Glicksman's study [7] of the steady-state form of the PSD shows that the ratio $\langle\rho^3\rangle/\langle\rho\rangle$ varies slowly with volume fraction, and remains of unit order. Their result implies that the diffusion screening length in Eq. (6), at least at small volume fractions, should be proportional to $V_V^{-1/2}$ in finite systems, and the coarsening rate constant relative to that of the LSW theory should increase approximately as $V_V^{1/2}$—both key predictions that may be tested directly by experiment. Carlow *et al.* [24] also obtained similar predictions earlier through estimation.

Following the classical LSW approach [1], the distribution function $F(\rho,\tau)$ satisfies the continuity equation

$$\frac{\partial F(\rho,\tau)}{\partial \tau} + \frac{\partial}{\partial \rho}\left(\frac{d\rho}{d\tau}F(\rho,\tau)\right) = 0. \tag{7}$$

The Mullins hypothesis of statistical self-similarity can be applied in the late stages of phase coarsening [25]. The distribution function achieves an affine form insofar as $F(\rho,\tau)$ may be recast in a product-function form, specifically as $F(\rho,\tau)=G(\rho)H(\tau)$. Here the function $H(\tau)$ is the time-dependent portion of the distribution function that specifies its temporal behavior, however, its explicit form is not important here. $G(\rho)$ is the time-independent, normalized PSD and satisfies the following equation:

$$\frac{d}{d\rho}\left(\frac{d\rho}{d\tau}\right) + \frac{1}{G(\rho)}\frac{d\rho}{d\tau}\frac{dG(\rho)}{d\rho} = \lambda, \tag{8}$$

where λ is the separation constant, or eigenvalue. The general solution to Eq. (8) is

$$G(\rho) = \frac{A}{d\rho/d\tau}\exp\left[\int_0^\rho \frac{1}{d\rho/d\tau}d\rho\right], \tag{9}$$

where we have absorbed λ into the normalization constant A determined by the normalization condition of the PSD. As shown in Eq. (9) the normalized PSD can be obtained from Eq. (9), provided that the growth rate $d\rho/d\tau$ is known. Before one attempts to calculate the PSD from Eq. (9), however, one must determine the constant $K^\star$ appearing in the growth rate equation (3).

Lifshitz and Slyozov [1] proved that steady-state solutions to Eq. (8) are possible if and only if $K^\star$ remains constant, the value of which may be determined by applying stability con-

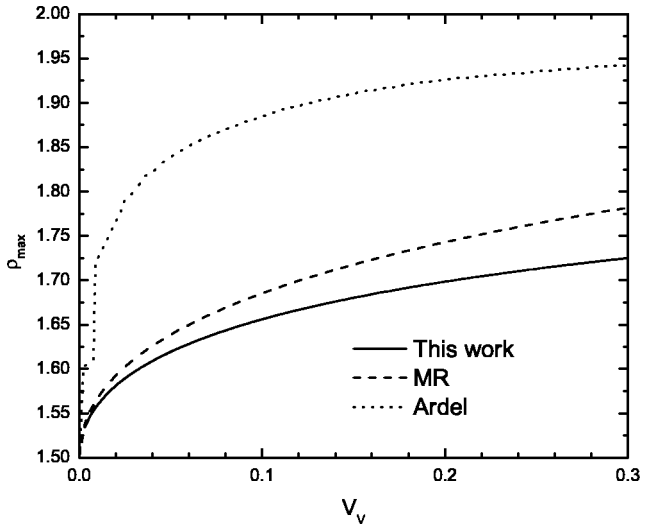

FIG. 1. The relationship between the normalized maximum radius ρ_{max} and volume fraction V_V. The present work is compared with the results from the theories of Ardell [3] and Marqusee and Ross (MR) [9].

ditions in ρ space. Specifically, Lifshitz and Slyozov showed that stability based on mass conservation in ρ space is achieved when two conditions are simultaneously satisfied:

$$\left.\frac{d\rho}{d\tau}\right|_{\rho=\rho_{max}} = 0, \quad \text{and} \quad \left.\frac{d}{d\rho}\left(\frac{d\rho}{d\tau}\right)\right|_{\rho=\rho_{max}} = 0. \tag{10}$$

Furthermore, application of these stability conditions lead to the following two results for the coarsening rate constant and the maximum particle radius:

$$K^* = \frac{2-(1-1/\rho_0)(1-\rho_0+\sqrt{\rho_0^2+\rho_0+1})}{(1-\rho_0+\sqrt{\rho_0^2+\rho_0+1})^3} \tag{11}$$

and

$$\rho_{max} = 1-\rho_0+\sqrt{\rho_0^2+\rho_0+1}. \tag{12}$$

Equations (11) and (12), respectively, relate the rate constant $K^\star$ and the maximum radius ρ_{max} directly to the normalized diffusion screening length, and hence directly to the interactions occurring among the particles. Applying the relationship between the diffusion screening length and the volume fraction, Eq. (6), to Eq. (12), and approximating $\langle\rho^3\rangle/\langle\rho\rangle \approx 1$, one may relate the maximum particle radius in the population directly to the volume fraction as

$$\rho_{max} = 1-\frac{1}{\sqrt{3V_V}}+\sqrt{\frac{1}{3V_V}+\frac{1}{\sqrt{3V_V}}+1}. \tag{13}$$

We note that Ardell predicted the relationship between the maximum radius of a coarsening particle to the volume fraction using his model [3], as did Marqusee and Ross with theirs [9]. A comparison of the maximum radius of a coarsening particle predicted from the current diffusion screening approach with those by Ardell and by Marqusee and Ross are plotted in Fig. 1 as a function of the microstructure's volume fraction. Indeed, as $V_V \to 0$, the asymptotic limit is approached, viz., $\rho_{max} \to 1.5$, recapturing the classical result obtained by LSW [1]. Different approximations used in the present theory and those employed by Ardell and Marqusee and Ross result in the detailed differences exhibited in Fig. 1. The important issue, however, from the standpoint of improving our understanding of the physics of microstructure evolution, is that such theoretical predictions can stimulate additional experimental studies to test them.

It is easier to measure experimentally the *average* radius $\langle R\rangle$ and thus implement the kinetic coarsening equation in terms of average radius rather than critical radius. Combining Eq. (4) with the definition of the normalized radius, one obtains the kinetic coarsening equation (14) in terms of the average radius,

$$\langle R(t)\rangle^3 - \langle R(0)\rangle^3 = 3K(V_V)t, \tag{14}$$

where

$$K(V_V) = 3K^\star\langle\rho\rangle^3. \tag{15}$$

$\langle R(0)\rangle$ is the average radius at $t=0$, and $K(V_V)$ is the coarsening rate constant at a volume fraction V_V. The ratio of $K(V_V)$ to $K(0)$, where $K(0)=8/9$ [1], can therefore be expressed as

$$\frac{K(V_V)}{K(0)} = \frac{27}{8}K^*\langle\rho\rangle^3. \tag{16}$$

Inserting Eq. (11) into Eq. (16) yields the relationship between the relative coarsening rate and the key microstructural length scales,

$$\frac{K(V_V)}{K(0)} = \frac{27}{8}\left[\frac{2-(1-1/\rho_0)(1-\rho_0+\sqrt{\rho_0^2+\rho_0+1})}{(1-\rho_0+\sqrt{\rho_0^2+\rho_0+1})^3}\right]\langle\rho\rangle^3. \tag{17}$$

Equation (17) specifically shows that the influence of volume fraction on the coarsening rate occurs through the diffusion screening length ρ_0 and the cube of the average normalized radius $\langle\rho\rangle$. The proportionality between the relative coarsening rate $K(V_V)/K(0)$ and the cubed average normalized radius was confirmed previously both by Brailsford and Wynblatt [6] and by Ardell [3]. On this point, interestingly, the three theories agree. However, the proportionality coefficient is a complicated function of the volume fraction, and does differ among the three theories. The differences among these coarsening theories is shown in Fig. 2. Figure 2 also suggests that the present prediction is between 6% and 16%, respectively, below independent computations carried out by Mandyam *et al.*, who used both "snapshot" and dynamic simulations in the range of volume fractions 0.1–0.3. [11]. The computer simulations by Mandyam *et al.* included interactions among particles [11], whereas those by Akaiwa and Voorhees [16] included both interactions and spatial correlations. The relative coarsening rates predicted from Marsh and Glicksman's field cell model [7] are between 17% and 39% higher than the present theoretical findings, 8–18% higher than the simulation results [11,16] and between 4%

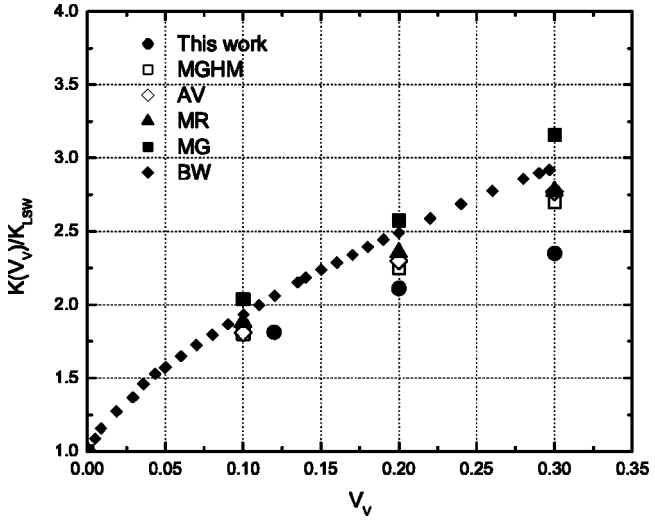

FIG. 2. Coarsening rates $K(V_V)$ normalized by the LSW coarsening rate K_{LSW} vs volume fraction V_V. The present work is compared with results from other theories (all solid symbols) Brailsfordand and Wynblatt [6], Marqusee and Ross [9], and Marsh and Glicksman [7]. Simulation results (all open symbols) of Akaiwa and Voorhees [16] and Mandyam *et al.* [11] are also shown.

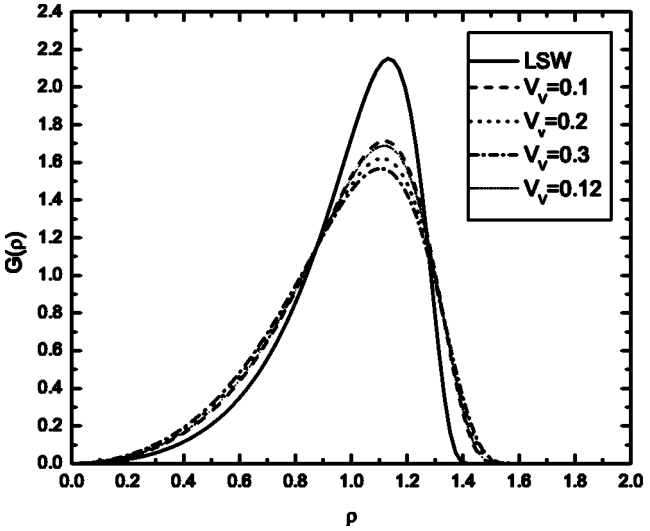

FIG. 3. Particle size distributions derived from screening theory (present work), $G(\rho)$, versus normalized radius ρ for several volume fractions, $V_V=0.1,0.12,0.2,0.3$. The $G(\rho)$ function from LSW theory ($V_V=0$) is shown for comparison.

and 10% higher than the predictions by Brailsford and Wynblatt [6]. In addition, theoretical predictions for the growth rates of the average particle from models III and VI of Tsumuraya and Miyata are four to five times larger than those predicted by the present work, and all the other theoretical, simulated, and experimental results. Ardell's coarsening rates [3] are also higher (by factors of 3–4) than are the other theoretical, simulation, and experimental results. These comparisons imply that Ardell and Tsumuraya and Miyata overestimated the contributions from the interactions among particles to the average growth rate. Because of the large disparity the coarsening rates predicted from Tsumuraya and Miyata, and Ardell, are not included in Fig. 2.

Figure 3 shows the PSD derived from the present theory for various values of V_V, from 0 to 0.3, all of which are obtained by numerical solution of Eq. (9) with the approximation, $\langle\rho^3\rangle/\langle\rho\rangle\approx 1$, for calculation of the normalized diffusion screening length ρ_0. After obtaining PSD's for various volume fractions, we calculated the ratio, $\langle\rho^3\rangle/\langle\rho\rangle$, for different volume fractions to check the approximation. We found that the ratio varies extremely slowly with volume fraction, but remains about 12% different from unity. These results from some PSD's will be compared with our own simulations and experimental results in Sec. IV.

III. SIMULATION

A two-phase coarsening system may be simulated by placing n particles of the dispersoid phase in a cubic box. The contiguous spaces between the particles are filled by the matrix phase, throughout which the dispersoid population is embedded. Particles are located by specifying the positions of their centers with three random coordinates representing the Cartesian vectors $\vec{\mathbf{r}}_i$ and by their radii R_i chosen initially from a relatively narrow Gaussian distribution.

Some additional simplifying assumptions are needed: (i) the kinetics of coarsening is determined solely by volume diffusion through the matrix; and (ii) the diffusion transport to or from each phase domain occurs slowly enough to be considered quasistatic. In the simulation, we use Laplace's equation as the quasistatic approximation to describe the multiparticle concentration fields in the matrix, so that

$$\nabla^2\mathcal{C}(\vec{\mathbf{r}}) = 0, \tag{18}$$

where $\mathcal{C}(\vec{\mathbf{r}})$ is the dimensionless concentration of the Laplacian diffusion field. The boundary conditions at the spherical interface of the ith particle are specified through the Gibbs-Thomson local equilibrium solubility relation, namely

$$\mathcal{C}(R_i) = \frac{1}{R_i}. \tag{19}$$

The solution to Laplace's equation for n particles may be represented as the superposition of n dimensionless concentration fields summed over the system of particles, namely,

$$\mathcal{C}(\vec{\mathbf{r}}) = \sum_{i=1}^{n} \frac{B_i}{|\mathbf{r}-\mathbf{r_i}|} + \mathcal{C}_\infty. \tag{20}$$

The ith particle's total volume flux $4\pi B_i$ and the far-field potential $\mathcal{C}_\infty$ comprise $n+1$ unknowns. The microstructure's global mass conservation law for a discrete system consisting of n spherical particles may be expressed through the volume fluxes as $\Sigma_{i=1}^{n} B_i=0$. Using Eq. (20) along with the mass conservation law, one obtains after a few steps of algebra

$$\mathcal{C}_\infty = \frac{1}{\langle R\rangle} - \frac{1}{n\langle R\rangle}\sum_{k=1}^{n} B_k \sum_{j\neq k}^{n} \frac{R_j}{r_{jk}}, \tag{21}$$

where r_{jk} is the distance between the centers of any pair of particles j and k. The relationship for the far-field potential, Eq. (21), expresses microstructure responses that include interactions among particles. Equation (21) clearly demonstrates that the far-field potential $\mathcal{C}_\infty$ depends explicitly on *local* information concerning particle positions and the distances between particle pairs. Moreover, Eq. (21) includes enough detailed environmental information to describe the "locale" of every particle, and, most importantly, its subtle influence on the particle's diffusion-limited growth or shrinkage.

The volume flux entering or leaving the surface of each particle may be related to the kinematics of the rate of change of spherical volume, to yield the dimensionless form of the growth rate of the ith particle,

$$\frac{dR_i}{dt} = -\frac{B_i}{R_i^2} \quad (i = 1,2,\ldots,n). \tag{22}$$

The Runge-Kutta method was used to integrate the growth rate, Eq. (22). One obtains a system of linear equations by substituting Eq. (20) into the Gibbs-Thomson boundary condition, Eq. (19), for the population of n particles. The set of linear equations may be cast in matrix form as

$$\mathbf{A}' \cdot \mathbf{B}' = \mathbf{U}', \tag{23}$$

where $\mathbf{A}'$, $\mathbf{B}'$, and $\mathbf{U}'$ are, respectively, $n\times n$, $n\times 1$, and $n\times 1$ matrices. These matrices are detailed in the Appendix. The Gauss-Seidel method was employed to solve the resultant system of linear equations, Eq. (23), yielding at each time step updated values for the B_i's. Substitution of the updated B_i's back into Eq. (22) dynamically advances (marches) the coarsening by sequentially updating both the radii of all the particles and their coordinates at any time step. The environmental information built into Eq. (21) adds important microstructural physics to the diffusion solution in the form of correlations. In fact, in the present simulations, one can calculate all terms exactly in Eq. (21), which means that one can calculate all the interactions for every particle. Normally mean-field descriptions of microstructure evolution are unable to calculate all interactions included in Eq. (21).

We carried out simulations of late-stage coarsening for various values of the volume fraction of the dispersoid phase from 10^{-10} to 0.2. The PSD's observed for volume fractions $V_V = 0.001, 0.01, 0.12$ are plotted in Fig. 4, which shows that the height of a PSD is gradually reduced and its width commensurately broadened with increasing volume fraction.

The growth law for particles for a dispersoid volume fraction of $V_V = 0.12$ is plotted in Fig. 5. The double logarithmic plot, Fig. 5, clearly shows that, after some transient period, a steady-state growth law develops where the cubic average radius of particles becomes proportional to the time. The coarsening rate constant of the cubic growth law is determined by the slope of $\langle R(t)\rangle^3$ vs t plot. The slope is calculated using a linear regression of these data. Using the definition of relative coarsening rate, the coarsening rate constant normalized by the coarsening rate constant of LSW, we obtained $K(0.12)/K(0) = 1.828$, which is close to the value, 1.814, derived from the present screening theory.

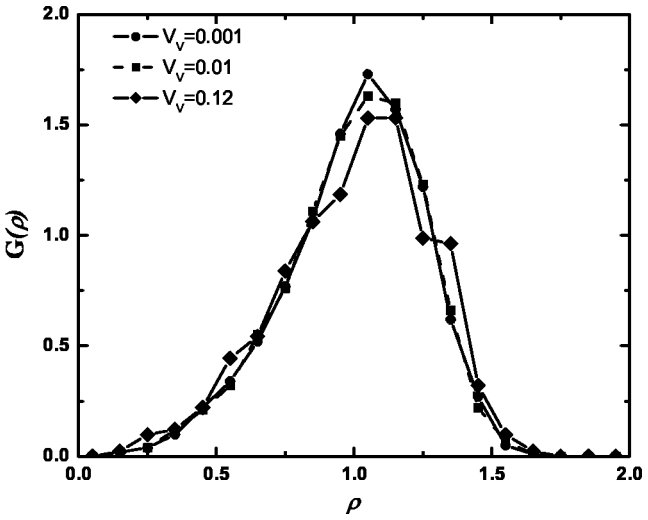

FIG. 4. Particle size distributions $G(\rho)$ derived from simulations based on the present work at $V_V = 0.001, 0.01, 0.12$. Increasing the volume fraction of the dispersoid lowers the peak value and broadens the PSD.

IV. COMPARISON WITH EXPERIMENT

Because the Al-Li system contains spherical precipitates with negligible strains at the particle-matrix interface, this binary alloy provides a nearly ideal system for studies of coarsening. Mahalingam *et al.* used quantitative transmission

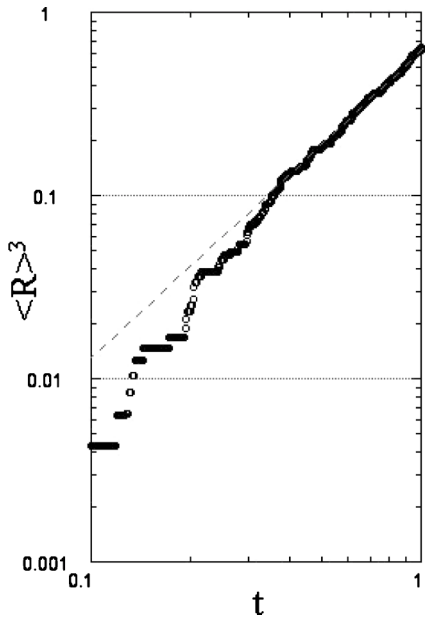

FIG. 5. Cube of the average particle dimensionless radius $\langle R\rangle^3$ vs dimensionless coarsening time (double logarithmic coordinates). Data are from the present simulations at the volume fraction $V_V = 0.12$.

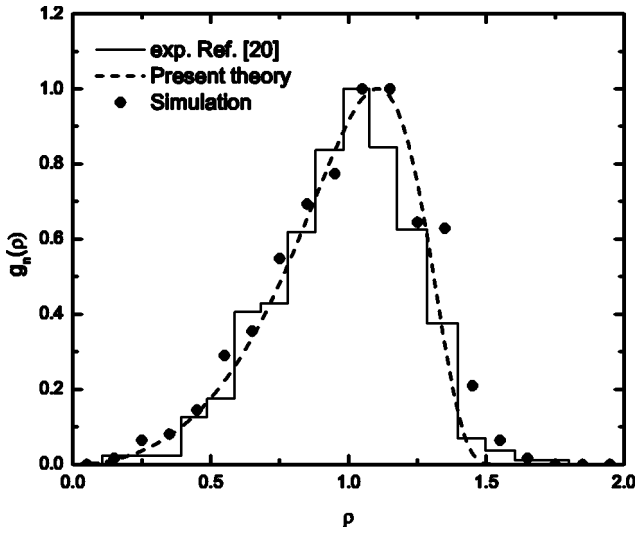

FIG. 6. Particle size distributions (normalized) $g_n(\rho)$ from present screening theory and simulations compared with the experimental PSD of Mahalingam *et al.* [20] for Al-Li alloy at a dispersoid volume fraction of $V_V=0.12$. The normalization used is to set the peak value, $g_n^{max}=1$, equal to unity.

electron microscopy [20] to investigate the coarsening behavior of δ' precipitates in a series of binary Al-Li alloys. These authors carried out careful experiments and obtained the microstructure's steady-state PSD. Mahalingam *et al.* claimed that only the PSD predicted from the theory of Davies *et al.* [26] is close to their experimental PSD for the case of volume fraction of δ' $V_V=0.12$, despite the fact that the other theories also predict a broadening of the PSD with increase of volume fraction of particles. Figure 6 shows the PSD's at volume fraction $V_V=0.12$ derived from the present theory and simulation, and from the experimental data of Mahalingam *et al.* [20]. Figure 6 shows that the PSD's from the present theory is in good agreement with the experimental PSD. We incorporated diffusional interactions among particles that yielded a new growth rate equation. When inserted into the continuity equation the new growth rate equation led to the PSD shown in Fig. 6. However, in their treatment of coarsening kinetics, Davies *et al.* used the LSW kinetic equation that lacks all particle-particle interactions, but added the influence of coalescence to the continuity equation. In fact, for the case of volume fraction $V_V=0.12$, Mahalingam *et al.* [20] specifically note that they did not observe any coalescence effects in their experiments. Although Davies *et al.* [26] predict a PSD in reasonable agreement with the recent experimental results, the mechanism responsible for the broadening of their PSD from that predicted by LSW is not applicable. In fact, diffusional interactions—i.e., "soft collisions" and not coalescences—among the particles, as explained in this paper, contribute most of the broadening to the PSD at lower volume fractions. In microstructures with much higher dispersoid volume fractions the effect of coalescence may become significant.

It is interesting to point out that the PSD derived from the present simulations is even closer to the experimental results of Mahalingam *et al.* [20] at volume fraction $V_V=0.12$. The reason for the better correspondence of our simulation-based PSD with experiment, as compared with continuum screening theory, is that in our simulations *all* the multiparticle interactions are included throughout the system. However, in modeling, one must approximate these interactions. In Fig. 6, it is demonstrated that the tail of the PSD derived from our simulations mimics the experimental data. We obtained an estimate for the maximum normalized radius using Eq. (13), and found at a volume fraction $V_V=0.12$ that $\rho_{max}\approx 1.67$. Using computer simulations, we found the corresponding maximum normalized radius $\rho_{max}\approx 1.74$. The experimental result reported by Mahalingam *et al.* shows that the corresponding maximum normalized radius $\rho_{max}\approx 1.80$ [20]. Figure 1 shows that at a dispersoid volume fraction of $V_V=0.12$, Marqusee and Ross's theory predicts $\rho_{max}\approx 1.70$, and Ardell's theory predicts $\rho_{max}\approx 1.90$.

In an attempt to calculate the relative kinetic coarsening rate, $K(0.12)/K(0)$, we obtained the following results from the continuum theory and simulation: $K(0.12)/K(0)=1.81$ and $K(0.12)/K(0)=1.83$, respectively, which are markedly different from the experimental value $K(0.12)/K(0)=3.72$ [20]. The value of the calculated coarsening rate is sensitive to the choice of the particle-matrix interfacial energy and the interdiffusion coefficient for the matrix, both of which remain uncertain. This suggests that one needs more extensive and accurate thermophysical data for experimental alloys used to test kinetic coarsening rate constants.

V. CONCLUSIONS

We approximated a two-phase microstructural system consisting of a spherical dispersoid phase randomly distributed within a matrix phase as a mesoscopic distribution of diffusion sources and sinks. Within the framework of a Poisson approximation for the quasistatic diffusion field, Yukawa solutions to the well-known Debye-Hückel equation may be used to describe the screened concentration fields surrounding the particles. The contributions of the effective interactions among a population of particles to the average growth rate of a particle was found. Such interactions increase the coarsening rate and alter in specific ways the PSD at any volume fraction $V_V \leqslant 0.3$. Computer simulations were carried out for various values of the dispersoid volume fractions using multiparticle diffusion techniques that exactly consider diffusional interactions among particles. Our results from modeling and simulation are in acceptable agreement with experimental results derived from Al-Li alloys.

Several additional specific conclusions can be drawn from this study:

(i) At small-to-moderate volume fractions of the precipitate phase $(0<V_V<0.3)$, the interaction screening length among particles is proportional to $V_V^{-1/2}$—a theoretical prediction which may now be tested through experiments.

(ii) Stronger interactions among particles reduce the height and broaden the steady-state PSD. Moreover, the present study established the relationship between the maximum radius of a particle and the volume fraction via Eq. (13). This too can be tested through experiment. At $V_V=0.12$, we found that the maximum normalized radius $\rho_{max}\approx 1.67$ from the continuum screening theory, and ρ_{max}

≈ 1.74 based on our multiparticle computer simulations. The experimental results of Mahalingham *et al.* show that in Al-Li two phase alloys, $\rho_{max} \approx 1.80$ at $V_V = 0.12$.

(iii) The relative coarsening rate, $K(V_V)/K(0)$, derived from screening theory is similar to that predicted by Brailsford and Wynblatt's theory [6], and is in reasonable agreement with recent multiparticle computer simulation results [11,16]. In the specific case where $V_V = 0.12$, the relative coarsening rate from screening theory agrees with multiparticle simulations reported here; however, the result differs by a factor of about 2 from experiment [20]. The difference might be related to the choice of particle-matrix interfacial energy and matrix interdiffusion coefficient used in the experimental study. More extensive and accurate thermophysical data are needed for experimental alloys used to test the coarsening rates derived from theory and simulation.

(iv) Estimates of the PSD's derived from modeling and simulation at $V_V = 0.12$ are in good agreement with the PSD derived from experimental results on Al-Li alloys [20]. We found that it is not neccessary to include coalescence effects at this relatively low volume fraction to predict an accurate PSD. Accurate description of interparticle interactions seems sufficient to obtain a PSD in good agreement with experiment, at least at lower volume fractions.

ACKNOWLEDGMENTS

The authors are pleased to acknowledge partial financial support received from the National Aeronautics and Space Administration, Marshall Space Flight Center, under Grant No. NAG-8-1468. The authors also gratefully acknowledge support from the National Science Foundation International Materials Institute program for the Combinatorial Sciences and Materials Informatics Collaboratory (CoSMIC-IMI) through NSF Grant No. DMR -0231291.

APPENDIX

Using terms and definitions already included in the body of this paper, matrices $\mathbf{A}'$, $\mathbf{B}'$, and $\mathbf{U}'$ in Eq. (23) are defined as follows:

$$\mathbf{A}' = \begin{pmatrix} \frac{1}{R_1} - \frac{1}{n\langle R\rangle}\sum_{j\neq 1}^{n}\frac{R_j}{r_{j1}} & \frac{1}{r_{12}} - \frac{1}{n\langle R\rangle}\sum_{j\neq 2}^{n}\frac{R_j}{r_{j2}} & \cdots & \frac{1}{r_{1n}} - \frac{1}{n\langle R\rangle}\sum_{j\neq n}^{n}\frac{R_j}{r_{jn}} \\ \frac{1}{r_{21}} - \frac{1}{n\langle R\rangle}\sum_{j\neq 1}^{n}\frac{R_j}{r_{j1}} & \frac{1}{r_2} - \frac{1}{n\langle R\rangle}\sum_{j\neq 2}^{n}\frac{R_j}{r_{j2}} & \cdots & \frac{1}{r_{2n}} - \frac{1}{n\langle R\rangle}\sum_{j\neq n}^{n}\frac{R_j}{r_{jn}} \\ \frac{1}{r_{31}} - \frac{1}{n\langle R\rangle}\sum_{j\neq 1}^{n}\frac{R_j}{r_{j1}} & \frac{1}{r_{32}} - \frac{1}{n\langle R\rangle}\sum_{j\neq 2}^{n}\frac{R_j}{r_{j2}} & \cdots & \frac{1}{r_{3n}} - \frac{1}{n\langle R\rangle}\sum_{j\neq n}^{n}\frac{R_j}{r_{jn}} \\ \cdot & \cdot & \cdots & \cdot \\ \cdot & \cdot & \cdots & \cdot \\ \cdot & \cdot & \cdots & \cdot \\ \frac{1}{r_{n1}} - \frac{1}{n\langle R\rangle}\sum_{j\neq 1}^{n}\frac{R_j}{r_{j1}} & \frac{1}{r_{n2}} - \frac{1}{n\langle R\rangle}\sum_{j\neq 2}^{n}\frac{R_j}{r_{j2}} & \cdots & \frac{1}{R_n} - \frac{1}{n\langle R\rangle}\sum_{j\neq n}^{n}\frac{R_j}{r_{jn}} \end{pmatrix}, \tag{A1}$$

$$\mathbf{B}' = \begin{pmatrix} B_1 \\ B_2 \\ B_3 \\ \cdot \\ \cdot \\ \cdot \\ B_n \end{pmatrix}, \tag{A2}$$

and

$$\mathbf{U}' = \begin{pmatrix} \frac{1}{R_1} - \frac{1}{\langle R \rangle} \\ \frac{1}{R_2} - \frac{1}{\langle R \rangle} \\ \frac{1}{R_3} - \frac{1}{\langle R \rangle} \\ \vdots \\ \frac{1}{R_n} - \frac{1}{\langle R \rangle} \end{pmatrix}. \tag{A3}$$

[1] I. M. Lifshitz and V. V. Slyozov, J. Phys. Chem. Solids **19**, 35 (1961).
[2] C. Wagner, Z. Elektrochem. **65**, 581 (1961).
[3] A. J. Ardell, Acta Metall. **20**, 61 (1972).
[4] J. H. Yao, K. R. Elder, Hong Guo, and M. Grant, Phys. Rev. B **45**, 8173 (1992).
[5] K. Tsumuraya and Y. Miyata, Acta Metall. **31**, 437 (1983).
[6] A. D. Brailsford and P. Wynblatt, Acta Metall. **27**, 489 (1979).
[7] S. P. Marsh and M. E. Glicksman, Acta Mater. **44**, 3761 (1996).
[8] M. E. Glicksman, *Diffusion in Solids, Field Theory, Solid-State Principles and Applications* (J. Wiley & Sons, New York, 2000).
[9] J. A. Marqusee and J. Ross, J. Chem. Phys. **80**, 536 (1984).
[10] V. E. Fradkov, M. E. Glicksman, and S. P. Marsh, Phys. Rev. E **53**, 3925 (1996).
[11] H. Mandyam, M. E. Glicksman, J. Helsing, and S. P. Marsh, Phys. Rev. E **58**, 2119 (1998).
[12] M. E. Glicksman, K. G. Wang, and S. P. Marsh, J. Cryst. Growth **230**, 318 (2001).
[13] J. Weins and J. W. Cahn, in *Sintering and Related Phenomena*, edited by G. C. Kuczynski (Plenum, New York, 1973), pp. 151–163.
[14] P. W. Voorhees and M. E. Glicksman, Acta Metall. **32**, 2013 (1984).
[15] C. W. J. Beenakker, Phys. Rev. A **33**, 4482 (1986).
[16] N. Akaiwa and P. W. Voorhees, Phys. Rev. E **49**, 3860 (1994).
[17] M. E. Glicksman, K. G. Wang, and P. Crawford, *Computational Modeling of Materials, Minerals and Metals Processing*, edited by Mark Cross *et al.* (TMS, Pennsylvania, 2001), pp. 703–713.
[18] M. E. Glicksman, K. G. Wang, and P. Crawford, Mater. Res. Innovations **5**, 231 (2002).
[19] A. Baldan, J. Mater. Sci. **37**, 2379 (2002).
[20] K. Mahalingam *et al.*, Acta Metall. **35**, 483 (1987).
[21] J. Alkemper, V. A. Snyder, N. Akaiwa, and P. W. Voorhees, Phys. Rev. Lett. **82**, 2725 (1999).
[22] V. A. Snyder, J. Alkemper, and P. W. Voorhees, Acta Mater. **48**, 2689 (2000).
[23] A. Baldan, J. Mater. Sci. **37**, 2171 (2002).
[24] G. R. Carlow, S. Yu. Krylov, and M. Zinke-Allmang, Physica A **261**, 115 (1998).
[25] W. W. Mullins, J. Appl. Phys. **59**, 1341 (1986).
[26] C. K. L. Davies, P. Nash, and R. N. Stevens, Acta Metall. **28**, 179 (1980).